Streamflow variability and optimal capacity of run-of-river hydropower plants

S. Basso[1] and G. Botter[1]

Received 20 February 2012; revised 22 August 2012; accepted 29 August 2012; published 12 October 2012.

[1] The identification of the capacity of a run-of-river plant which allows for the optimal utilization of the available water resources is a challenging task, mainly because of the inherent temporal variability of river flows. This paper proposes an analytical framework to describe the energy production and the economic profitability of small run-of-river power plants on the basis of the underlying streamflow regime. We provide analytical expressions for the capacity which maximize the produced energy as a function of the underlying flow duration curve and minimum environmental flow requirements downstream of the plant intake. Similar analytical expressions are derived for the capacity which maximize the economic return deriving from construction and operation of a new plant. The analytical approach is applied to a minihydro plant recently proposed in a small Alpine catchment in northeastern Italy, evidencing the potential of the method as a flexible and simple design tool for practical application. The analytical model provides useful insight on the major hydrologic and economic controls (e.g., streamflow variability, energy price, costs) on the optimal plant capacity and helps in identifying policy strategies to reduce the current gap between the economic and energy optimizations of run-of-river plants.

Citation: Basso, S., and G. Botter (2012), Streamflow variability and optimal capacity of run-of-river hydropower plants, *Water Resour. Res.*, *48*, W10527, doi:10.1029/2012WR012017.

1. Introduction

[2] Hydropower is one of the most important sources of renewable energy. However, less than one third of the available hydroelectric potential is currently exploited (British Hydropower Association, http://www.british-hydro.org/) and a significant development of small-scale hydropower plants (mini and micro hydroelectric) is expected in next decades [*Paish*, 2002].

[3] Most small hydropower plants are run-of-river plants, which have some key advantages over conventional storage plants: they are more flexible, better suited to small heads and they have smaller socioeconomic impacts. Conventional hydropower schemes rely on large dams which typically induce dramatic changes in the landscape (large areas are permanently inundated) and lead to significant alterations of the downstream flow regime [*Poff et al.*, 2007; *Zolezzi et al.*, 2009; *Botter et al.*, 2010]. Run-of-river hydropower plants, on the other hand, do not induce significant modifications of the landscape, and require only low weirs without reservoirs, thereby exerting a less intensive regulation of the incoming flows. Furthermore, in run-of-river plants the water volumes diverted are released back to the river relatively close to the intake. For the above reasons, run-of-river plants are generally considered more socially and environmentally acceptable.

[4] The overall environmental impact of run-of-river plants, though being smaller than that produced by dams, should not be underestimated. In fact, the water subtracted to the river may change significantly the hydrologic regime of the reaches between the intake and the outflow, and the weir built for the diversion can break the hydrological and ecological connectivity of the whole river network. As a result, relevant modifications of downstream habitat conditions (e.g., water temperature, sediment transport, nutrient and dissolved oxygen loads) can be observed, with local disturbances propagating along the river and producing notable large-scale impacts on the overall primary productivity and the riverine biodiversity [*Pringle*, 2001; *Freeman et al.*, 2007]. In the last decades of the previous century the concept of minimum flow discharge (*MFD*) has been introduced to set upward limits to the anthropogenic exploitation of water resources, and has been later adopted by water managers in many countries of Europe, North America and Australia [*Tharme*, 2003]. In most European countries the existing *MFD* prescriptions represent a significant constraint to the energy produced by run-of-river plants [*ARCADIS*, 2011].

[5] The amount of energy produced by a run-of-river hydropower plant mainly depends on the sequence of streamflows workable by the plant during its lifetime, which is controlled by the river flow availability. Streamflows observed at a river cross section strongly fluctuate in time at multiple timescales, mirroring the variability of complex hydroclimatic processes, chiefly the rainfall forcing. The streamflow variability has been portrayed by hydrologists and engineers

[1]Department ICEA and International Center for Hydrology "Dino Tonini," University of Padua, Padua, Italy.

Corresponding author: G. Botter, Department ICEA, University of Padua, via Loredan 20, IT-35131 Padua, Italy. (gianluca.botter@dicea.unipd.it)

0043-1397/12/2012WR012017

by means of the flow duration curve (FDC), or, alternatively, by the probability density function (pdf) of the streamflows. The shape of the duration curve places a substantial constraint on the optimal capacity (i.e., the maximum flow a plant can process) and other design attributes of a run-of-river plant, as demonstrated by the large number of studies on the subject (for a complete review, see *Bozorg Haddad et al.* [2011]). Early studies pertained to the use of the Lagrange Multipliers for the optimal choice of some design characteristics of the plant (e.g., penstock diameters, units number) to maximize the generated energy and/or the investment return [e.g., *Fahlbuch*, 1983, 1986; *Da Deppo et al.*, 1984; *Najmaii and Movaghar*, 1992]. The direct utilization of flow duration curves for the design of small hydropower plants was also proposed by *Vogel and Fennessey* [1995] on a graphical basis. More recently, flow duration curves have been extensively used in numerical studies to identify optimal plant attributes and evaluate the impacts of technological and economic constraints on the viability of small hydropower projects. *Voros et al.* [2000] developed an empirical shortcut design method to select the capacity maximizing the economical benefit of the investment. *Montanari* [2003] proposed a new method to address the choice of the turbine type for low-head sites. More recently, *Anagnostopoulos and Papantonis* [2007] carried out a multiobjective optimization which accounted for the economic benefits of the investment and the degree of exploitation of the available potential. Similarly, *Santolin et al.* [2011] tested different technical and economic criteria to determine the available design solutions for a plant and compare their feasibility and performance. All these studies made use of numerical algorithms to maximize suitable objective functions defining the target of the optimization.

[6] In contrast to all previous works, the present paper provides analytical expressions for the plant capacity which optimizes the produced energy and the economic profitability of a hydropower plant, taking into account the effect of the natural streamflow variability and downstream flow requirements. The relevance of the study stems from the generality and the simplicity of the proposed formulation, which encompasses all possible climate regimes, turbine types and catchment sizes. The framework developed gives insight on the dependence of the optimal plant capacity on economic, hydromechanical and hydrologic factors (in particular the underlying streamflow variability), and helps in identifying policies aimed at bridging the gap between the economic and energy optimization of a plant.

2. Optimizing the Energy Production in a Run-of-River Plant

[7] In our mathematical derivation, for the sake of simplicity we shall focus on a plant equipped with a single turbine, where the hydropower plant capacity is taken as the only decision variable, thereby assuming the remaining design attributes of the plant to be known or derivable on the basis of the capacity. The energy produced by a hydropower plant during a time period ΔT is the time integral of the time-dependent power generated during ΔT:

$$E(Q) = \rho g\, \eta_P \int_0^{\Delta T} H(t)\, \eta\left(\frac{q_w(t)}{Q}\right) q_w(t)\, dt \qquad (1)$$

where Q is the plant capacity (i.e., design flow), q_w is the processed flow, ρ is the water density, g is the standard gravity, η_P is the efficiency of the plant, η is the turbine efficiency (dependent on the turbine type and on the ratio $x = q_w/Q$) and H is the net hydraulic head (the difference between the gross hydraulic head and the energy losses within the plant). Following *Najmaii and Movaghar* [1992], *Voros et al.* [2000], *Montanari* [2003], *Anagnostopoulos and Papantonis* [2007], and *Santolin et al.* [2011], in the forthcoming calculations we shall assume the head H to be a constant (hence neglecting both the head losses and possible reductions of the gross head for incoming flows larger than Q).

[8] For time periods ΔT much longer than the correlation scale of the streamflows [*Botter*, 2010] (e.g., a few years, a decade, the lifetime of the plant), the incoming streamflows can be assumed to be ergodic, and the frequencies characterizing the different values of q_w in equation (1) are described by the probability density function of the workable flows, p_w. Therefore, the time integral of equation (1) can be replaced by a weighted integral over q_w, the weighting factor being p_w:

$$E(Q) = \Delta T\, H\, \rho g\, \eta_P \int_0^{\infty} \eta\left(\frac{q_w}{Q}\right) p_w(q_w)\, q_w\, dq_w. \qquad (2)$$

To further specify equation (2), we need to know the operation of a run-of-river power plant (Figure 1) and to express the pdf of the flows processed by the plant, $p_w(q_w)$, in terms of the pdf of the incoming streamflows $p(q)$ (Figure 2). Due to flow requirements downstream of the intake, the flow which can be diverted from a river to the plant is the difference between the incoming streamflow q and the *MFD* (when such difference is positive). Moreover, the actual range of streamflows processed by the plant depends on the technical constraints of the turbine, namely its capacity Q, and the minimum workable flow Q_C (i.e., cutoff flow), which is usually expressed as a fraction of Q (i.e., $Q_C = \alpha_C Q$). In particular, when the flow which could be diverted ($q - MFD$) is lower than the cutoff flow Q_C, it cannot be processed and $q_w = 0$. This happens with probability $1 - D(Q_C + MFD)$, $D(\cdot)$ being the duration curve of the inflows (i.e., $D(z) = \int_z^{\infty} p(q)dq$). On the other hand, when the diverted flows are in between the cutoff flow and the capacity of the plant, they are entirely processed by the plant, and $q_w = q - MFD$. Finally, when the flow which could be diverted exceeds the capacity of the plant, only the flow Q is actually taken from the river and processed. This happens with a probability equal to $D(Q + MFD)$. The pdf of the flows which are processed by the plant hence corresponds to the incoming streamflow pdf p (dashed line in Figure 2) simply translated leftward by a value equal to the *MFD*, with the two tails of the original distribution becoming two atoms of probability associated to $q_w = 0$ and $q_w = Q$ (Figure 2). The probability distribution of the workable flows $p_w(q_w)$ can thus be expressed as

$$p_w(q_w) = p(q_w + MFD) \text{ if } \alpha_C Q < q_w < Q \qquad (3)$$

while for $q_w = 0$ and $q_w = Q$ we have two atoms of probability respectively equal to $[1 - D(\alpha_C Q + MFD)]$ and

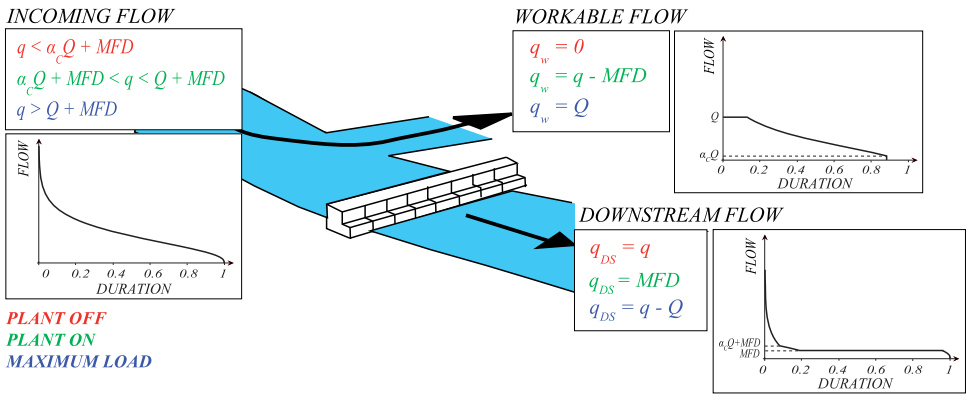

Figure 1. Scheme of the functioning of a run-of-river hydropower plant. Here q is the incoming streamflow, q_w is the workable flow, q_{DS} is the flow downstream the plant intake, MFD represents the flow requirements downstream the plant intake, Q is the design flow, and $\alpha_C Q$ is the cutoff flow. Red, green, and blue symbols describe the operation of the plant when it is turned off, turned on, and working at its maximum load, respectively. The duration curve of incoming streamflows and the resulting duration curves of workable and downstream flows are also represented.

$D(Q + MFD)$. When the expression of the workable flow pdf given by equation (3) is used, equation (2) becomes

$$E(Q) = \Delta T\, H\, \rho g\, \eta_P \left[\int_{\alpha_C Q}^{Q} \eta\left(\frac{q_w}{Q}\right) p(q_w + MFD)\, q_w\, dq_w + \eta(1)\, Q\, D(Q + MFD) \right]. \quad (4)$$

The second term within the square brackets on the right-hand side of equation (4) is originated from the atom of probability in correspondence of $q_w = Q$, while the first term derives from the continuous part of the workable flow pdf. The maximization of the produced energy $E(Q)$ requires to specify the efficiency function $\eta(x)$. The efficiency pertaining to each turbine type can be represented by means of specific curves characterized by distinctive shapes and working ranges. Examples of efficiency curves for different types of turbines [*European Small Hydropower Association*, 1998] are displayed with thick gray lines in Figure 3. The actual turbine efficiency curve will be first approximated by a step function (section 2.1) and then by a piecewise linear function (section 2.2). The former case is used primarily for illustrative purposes.

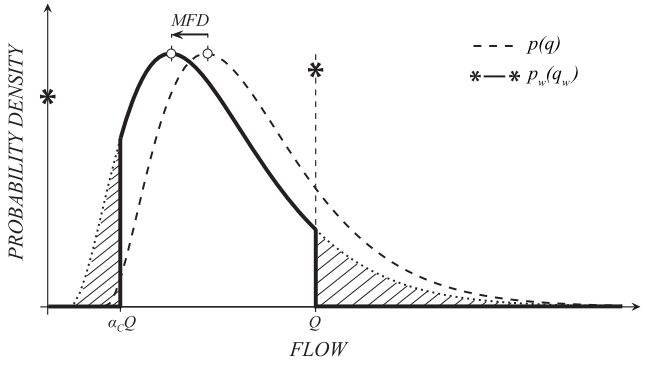

Figure 2. Probability distributions of streamflows ($p(q)$, dashed line), of river flows which can be diverted (dotted line), and of flows workable by an hydropower plant ($p_w(q_w)$, solid line and stars). The pdf of river flows which can be diverted (dotted line) is derived by a translation of the streamflow pdf (dashed line) equal to MFD. Q is the design flow of the turbine (i.e., the maximum flow workable by the plant), and $\alpha_C Q$ is the cutoff flow of the turbine (i.e., the minimum flow workable by the plant). The dashed areas represent the probabilities of flows lower than $\alpha_C Q$ and greater than Q, respectively, which become atoms of probability to have workable flows equal to zero and Q (represented with stars in the workable flow pdf).

2.1. Turbine Efficiency Represented by a Step Function

[9] When the turbine efficiency for different values of x is described by means of a step function, the following expression holds:

$$\eta(x) = \begin{cases} 0 & \text{if } x < \alpha \\ \eta_M & \text{if } x \geq \alpha \end{cases} \quad (5)$$

where α is a critical value of the ratio x (dependent on the turbine type) suitably chosen between α_C and α_M to provide the best fit between the actual efficiency curve and the step function model (Figure 3). By inserting equation (5) into equation (4) we obtain

$$E(Q) = \Delta T\, H\, \rho g\, \eta_P\, \eta_M \left[\int_{\alpha Q}^{Q} p(q_w + MFD)\, q_w\, dq_w + Q\, D(Q + MFD) \right]. \quad (6)$$

The maximum of the function $E(Q)$ can be found by computing its derivative with respect to Q using the Leibniz integral rule. From equation (6) after some manipulations (see Appendix A) we obtain

$$\frac{dE}{dQ} = \Delta T\, H\, \rho g\, \eta_P\, \eta_M [D(Q + MFD) + \alpha Q\, D'(\alpha Q + MFD)]. \quad (7)$$

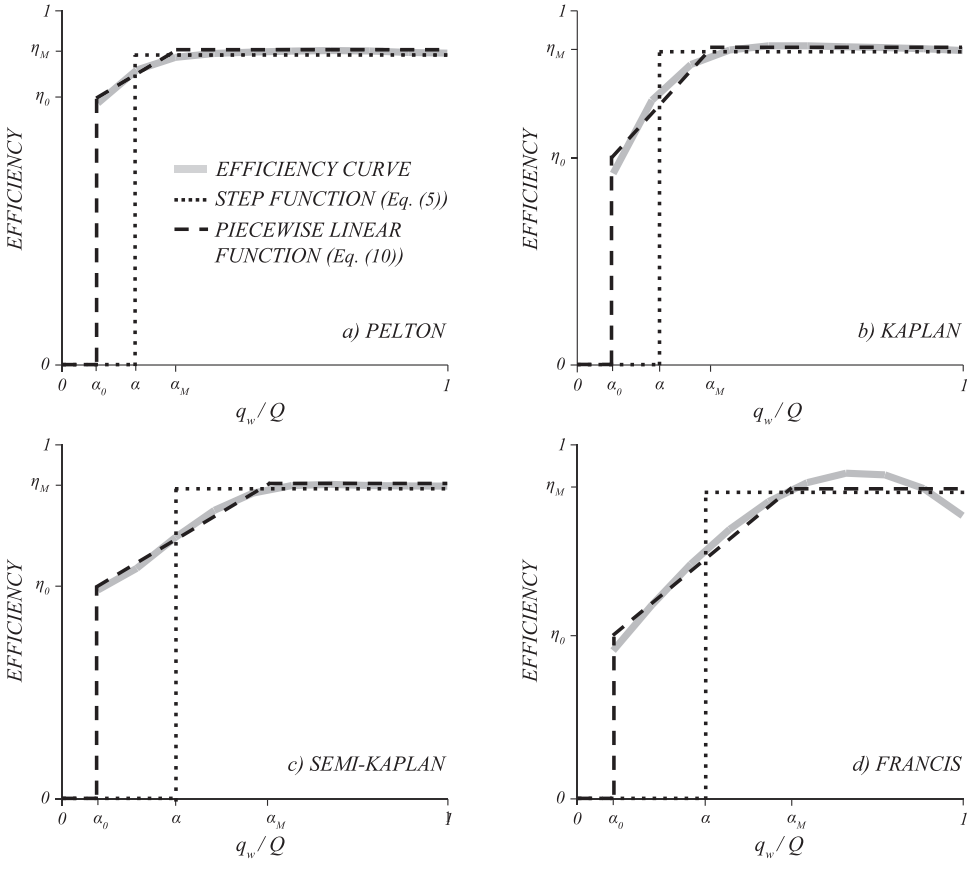

Figure 3. Efficiency curves for different turbine types (solid gray lines), taken from the literature [*European Small Hydropower Association*, 1998]. The efficiency curves display the efficiency of the turbine as a function of the ratio between the working flow rate q_w and the design flow Q. The approximation of the efficiency curves given by the step (dotted lines, equation (5)) and the piecewise linear (dashed lines, equation (10)) functions are displayed for the different cases, with the validity boundaries of the different parts of these functions (α, α_0, and α_M) and the corresponding efficiency values (η_0 and η_M).

To evidence the physical meaning of equation (7), we focus on the terms within the square brackets and express the infinitesimal variation of energy dE produced by an infinitesimal increment of the capacity dQ:

$$dE \propto D(Q + MFD)\, dQ + \alpha Q\, D'(\alpha Q + MFD)\, dQ. \qquad (8)$$

The first term on the right-hand side of equation (8) is the product between the percentage of time during which the design flow Q is processed and the increment of the capacity, dQ. Hence, this term represents the rise of processed volumes due to increased plant size (top dashed area in Figure 4). The second term (which is negative because $D'(z) = -p(z) < 0$) is the product between the value of the lower limit of the workable flows, αQ, and the decrease of its duration, which is obtained computing the product between dQ and the derivative of the duration curve evaluated in $\alpha Q + MFD$, $D'(\alpha Q + MFD)$. This second term thus represents the loss of processed volumes (bottom dashed area in Figure 4) due to the increase of the minimum workable flow Q_C.

[10] The condition providing the design flow which maximizes the energy production, Q_{EN}, can be obtained by setting $dE/dQ = 0$ in equation (7), and expressing D' in terms of p. Hence, Q_{EN} must adhere to the following equation:

$$D(Q_{EN} + MFD) = \alpha^2 Q_{EN}\, p(\alpha Q_{EN} + MFD). \qquad (9)$$

Equation (9) states that Q_{EN} is the capacity in correspondence of which the marginal increment of energy production due to increased capacity is balanced by the marginal loss of energy generated by the lowest flows, induced by the corresponding increase of the cutoff flow Q_C. The optimal capacity of the plant can be easily derived via a graphical method, by plotting the functions appearing at the two sides of equation (9). The left-hand side monotonically decreases from 1 to 0 according to the duration curve of the inflows translated by the *MFD*. The right-hand side, instead, is typically bell shaped, with the position and the intensity of the peak being dependent on the underlying streamflow variability. Both theoretical arguments [*Botter et al.*, 2007] and observational evidences show that the function $Q\,p(\alpha Q + MFD)$ takes relatively constant values (<2) for highly variable regimes, but becomes peaked (with the maximum typically not exceeding 5) when the

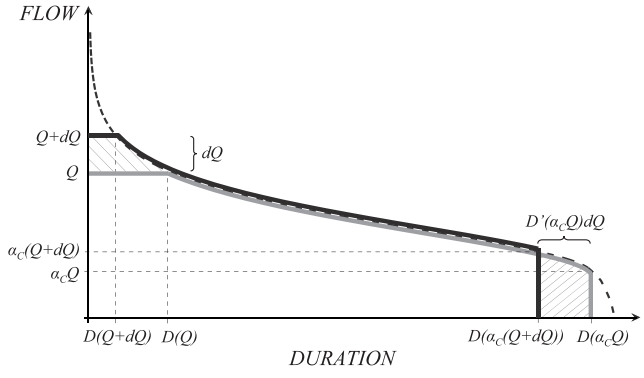

Figure 4. Duration curves of the streamflows (dashed line) and of the flows workable by an hydropower plant (solid lines). The gray line is the duration curve of the flows workable by a hydropower plant with capacity Q, while the black line is the duration curve of the workable flows due to an increment dQ of the plant capacity. For simplicity and without any loss of generality, we assumed $MFD = 0$ in this representation. The top dashed area represents the new water volume worked by the plant due to an increment dQ of the design flow Q, while the bottom dashed area represents the water volume the plant no longer works due to the increase of the minimum flow workable by the turbine induced by the increase of the design flow Q.

flow variability is reduced (see section 5). Provided that $\alpha \simeq 0.1$, the intersection between the two sides of equation (9) can hence be observed only when $D(Q_{EN} + MFD) < 0.05$. When $MFD \ll Q_{EN}$ (as observed in most circumstances), then $D(Q_{EN} + MFD) \simeq D(Q_{EN})$. This also implies that the duration of the optimal capacity, $D(Q_{EN})$, should satisfy the condition $D(Q_{EN}) < 0.05$ (see Figure 10). The latter seems to be a useful operational rule to set a boundary for Q_{EN} in practical application.

2.2. Turbine Efficiency Represented by a Piecewise Linear Function

[11] Piecewise linear functions often provide a more realistic description of the actual shape of the efficiency curves if compared with step functions (Figure 3). In this case, the analytical expression of the efficiency function η is

$$\eta(x) = \begin{cases} 0 & \text{if } x < \alpha_0 \\ \dfrac{x - \alpha_0}{\alpha_M - \alpha_0}(\eta_M - \eta_0) + \eta_0 & \text{if } \alpha_0 \le x < \alpha_M \\ \eta_M & \text{if } x \ge \alpha_M \end{cases} \tag{10}$$

which substituted into equation (4) yields

$$E(Q) = \Delta T\, H\, \rho g\, \eta_P \left\{ \int_{\alpha_M Q}^{Q} \eta_M\, p(q_w + MFD)\, q_w\, dq_w + \eta_M\, Q\, D(Q + MFD) + \int_{\alpha_0 Q}^{\alpha_M Q} \left[\frac{q_w - \alpha_0 Q}{\alpha_M Q - \alpha_0 Q}(\eta_M - \eta_0) + \eta_0 \right] p(q_w + MFD) q_w dq_w \right\}. \tag{11}$$

Equation (10) shows that flows greater than $\alpha_M Q$ are processed with the maximum efficiency η_M, while flows in the range between $\alpha_0 Q$ and $\alpha_M Q$ are characterized by suboptimal efficiencies, linearly increasing from η_0 (for $q_w = \alpha_0 Q$) to η_M (for $q_w = \alpha_M Q$). The maximum of the function $E(Q)$ can be found by computing dE/dQ and setting it equal to zero. Using the Leibniz integral rule, after some manipulations (see Appendix A) we obtain:

$$\frac{dE}{dQ} = \Delta T\, H\, \rho g\, \eta_P \left[\eta_M\, D(Q + MFD) + \eta_0\, \alpha_0\, Q\, D'(\alpha_0 Q + MFD) + \int_{\alpha_0}^{\alpha_M} \left(\frac{\eta_M - \eta_0}{\alpha_M - \alpha_0}\, x \right) Q x\, D'(Qx + MFD)\, dx \right]. \tag{12}$$

Similarly to equation (7), the physical meaning of equation (12) can be evidenced by focusing on the terms within the square brackets. To this end, let us express the infinitesimal variation of the energy produced by an infinitesimal increment of the capacity as

$$dE \propto \eta_M\, D(Q + MFD)\, dQ + \eta_0\, \alpha_0 Q\, D'(\alpha_0 Q + MFD)\, dQ + \int_{\alpha_0}^{\alpha_M} \left(\frac{\eta_M - \eta_0}{\alpha_M - \alpha_0}\, x \right) Q x\, D'(Qx + MFD)\, dQ\, dx. \tag{13}$$

The first and second terms at the right-hand side of equation (13) can be interpreted analogously to the right-hand side of equation (8). The third term, instead, represents the reduction of the energy produced in the range of the suboptimal efficiencies $\eta_0 < \eta < \eta_M$, induced by the change of duration associated to the various efficiencies. According to equation (13), an increase of Q leads to an increase of E only if the energy obtained from the additional water volume processed exceeds the energy losses associated with the water volume the plant no longer works and the decrease of the energy produced in the range of suboptimal efficiencies. The condition providing the capacity which maximizes the produced energy, Q_{EN}, can be obtained by setting $dE/dQ = 0$ in equation (12). Therefore, Q_{EN} satisfies

$$\underbrace{D(Q + MFD)}_{f_{EN}} = \underbrace{-\frac{\eta_0}{\eta_M}\alpha_0 Q D'(\alpha_0 Q + MFD) - \int_{\alpha_0}^{\alpha_M} \left(\frac{1 - \eta_0/\eta_M}{\alpha_M - \alpha_0} \right) Q x^2 D'(Qx + MFD) dx}_{g_{EN}} \tag{14}$$

Equation (14) provides some insight on the typical value of $D(Q_{EN})$. In most cases, the integral term of the above equation can be neglected, mainly because the integrand function is usually small and the range of integration is relatively narrow. Hence, equation (14) can be simplified as follows:

$$D(Q+MFD) = \frac{\eta_0}{\eta_M}\alpha_0^2 Q p(\alpha_0 Q + MFD). \tag{15}$$

Equation (15) is very similar to equation (9), with the exception of a multiplier equal to $\eta_0/\eta_M < 1$ at the right-hand side. Hence, the same reasoning presented in section 2.1 to set a boundary for $D(Q_{EN})$ still holds, suggesting that $D(Q_{EN}) < 0.05$ in the general case.

3. Optimization Based on Economic Indices

[12] The revenues generated by a run-of-river hydropower plant can be calculated by multiplying the produced energy by the selling price of energy from renewable sources e_p, which is assumed here to be constant (as in most EU countries a feed-in tariff fixed by national laws exists to promote the production of energy from renewable sources). To make a proper economic assessment of the hydropower project, we shall assume hereafter that the ergodicity hypothesis underlying equation (4) can be applied within each year of ΔT, so as the annual revenue $R_1(Q)$ is the same every year. Hence, we can compute the annual proceeds $R_1(Q)$ as

$$R_1(Q) = e_p E_1(Q) \tag{16}$$

where $E_1(Q)$ is $E(Q)$ expressed by equation (11) with $\Delta T = 1$ year.

[13] The overall present value $R_n(Q)$ of every cash inflow occurring during n years (e.g., the duration of state incentives or the lifetime of the plant) can be computed by means of the following expression:

$$R_n(Q) = \sum_{k=1}^{n} \frac{1}{(1+r)^k} R_1(Q) = \frac{1}{r}\left(1 - \frac{1}{(1+r)^n}\right) R_1(Q) = \hat{r} R_1(Q) \tag{17}$$

where r is the (constant) annual discount rate and $\hat{r} = \frac{1}{r}\left(1 - \frac{1}{(1+r)^n}\right)$ is an auxiliary variable expressing the multiplier used to compute the present value of the overall cash inflows.

[14] Typically hydropower plants are characterized by initial investment costs much higher than the corresponding operation expenses [e.g., *Aggidis et al.*, 2010]. Therefore, we neglect the costs incurring during the functioning of the plant [e.g., *Fahlbuch*, 1983] to focus on the construction expenses. Several past studies have investigated the relation between construction costs and some key features of a hydropower plant, chiefly the nominal power and the hydraulic head [*Gordon and Penman*, 1979; *Gordon*, 1981; *Gordon*, 1983; *Gordon and Noel*, 1986; *Papantonis*, 2001; *Ogayar and Vidal*, 2009; *Aggidis et al.*, 2010]. Following the above papers, the construction costs are expressed as a function of the design flow (all the other terms being constants) as

$$C(Q) = a Q^b \tag{18}$$

where a and b are empirical coefficients. Typical values for a and b can be derived from previous studies or via empirical estimates of the relationship between construction costs and plant features [e.g., *Ogayar and Vidal*, 2009; *Aggidis et al.*, 2010]. While a can be highly variable from site to site, the parameter b has been found to be weakly variable around 0.6 in most cases [*Aggidis et al.*, 2010].

[15] The economic suitability of an investment for a run-of-river hydropower plant is evaluated by means of the maximization of two standard economic indices: the net present value (*NPV*) and the internal rate of return (*IRR*). Both the *NPV* and the *IRR* quantify the suitability of an investment, but while the *NPV* focuses on the expected wealth, the *IRR* focuses on the risk. Hence, maximizing the *NPV* dictates choosing the option that provides the maximum return, while *IRR* maximization would lead to choosing the lowest risk option. As such, the *IRR* analysis often leads to the choice of alternatives with relatively small investment costs. For this reason, the maximization of the *IRR* to select the optimal project among mutually exclusive alternatives has been questioned, suggesting the need to compute the internal rate of return on incremental investments between alternatives. However, to show an application of the analytical method developed in this paper, we limit our discussion to the maximization of the *IRR* of the total investment, which is also the starting point of more refined economic evaluations. The same type of analysis has been carried out also by *Kaldellis et al.* [2005], *Anagnostopoulos and Papantonis* [2007], and *Santolin et al.* [2011]. In contrast to all previous studies, however, in this paper the economic optimization is performed analytically, providing insight on the interplay between the economic and hydrological processes in determining the optimal capacity of a plant.

[16] The net present value of a sequence of cash inflows/outflows is defined as the sum of every cash flow discounted back to its present value. In this case all future cash flows are incoming flows (the proceeds obtained from the selling of the produced energy). Conversely, the only outflow occurs at time zero, and it is represented by the construction cost of the plant, evaluated here by assuming the plant could be completed during the first year and neglecting possible financings and the related interests. Hence, the *NPV* can be computed as

$$NPV(Q) = R_n(Q) - C(Q) = \hat{r} R_1(Q) - C(Q). \tag{19}$$

The condition providing the capacity which maximizes the *NPV*, Q_{NPV}, can be obtained by calculating $dNPV(Q)/dQ$ through equations (12), (16), (18) and (19), and setting it equal to zero. Q_{NPV} hence should satisfy

$$\underbrace{\left[\eta_M D(Q+MFD) + \eta_0 \alpha_0 Q D'(\alpha_0 Q + MFD) + \int_{\alpha_0}^{\alpha_M} \left(\frac{\eta_M - \eta_0}{\alpha_M - \alpha_0}\right) Q x^2 D'(Qx + MFD)\, dx\right] \hat{r} e_p H \rho g \eta_P}_{f_{NPV}} = \underbrace{a b Q^{b-1}}_{g_{NPV}}. \tag{20}$$

According to equation (20), the optimal design flow is achieved whenever the marginal revenues due to increased plant size (f_{NPV}) are equal to the corresponding marginal cost (g_{NPV}). The comparison of equations (14) and (20) shows that, as expected, $Q_{NPV} < Q_{EN}$ except when the costs of the plant are negligible. The optimal capacity Q_{NPV} can be obtained from the intersections between the functions $f_{NPV}(Q)$ and $g_{NPV}(Q)$ in equation (20). The behavior of $f_{NPV}(Q)$ is chiefly determined by the first term on the left-hand side because $\alpha_0 \ll 1$ and the integral term can often be neglected (see section 2.2). Hence, $f_{NPV}(Q)$ monotonically decreases to 0 according to the duration curve of the inflows, translated by the *MFD*. Meanwhile, $g_{NPV}(Q)$ display a power law behavior, with a rapid drop for very small values of Q (rapidly driving $g_{NPV}(Q)$ below $f_{NPV}(Q)$), followed by a plateau. Hence, in the range of discharges which could potentially be diverted from the river, g_{NPV} can be assumed to be roughly constant, e.g., equal to the value assumed in correspondence of Q_{EN}. Hence, equation (20) can be approximated as

$$D(Q_{NPV} + MFD) \simeq \frac{ab}{\hat{r}\, e_p\, H\, \rho g\, \eta_P \eta_M}\, Q_{EN}^{b-1} \tag{21}$$

which states that the duration of the sum of the optimal capacity Q_{NPV} and the *MFD* is equal to the ratio between the marginal cost of the plant evaluated for $Q = Q_{EN}$ and the annual revenues generated by processing a constant unit flow with the maximum efficiency. Equation (21) can be a useful tool to assess the approximate value of Q_{NPV}, depending on economic and hydrological attributes. Provided that b is nearly constant, the other technical and economic features of the project (the energy price, the head, the efficiency, the discount rate, the unit cost a) impact only the right-hand side of equation (21), and hence the duration of $Q_{NPV} + MFD$. The hydrological features of the site (streamflow regime and *MFD*), instead, chiefly modulate the relationship between $D(Q_{NPV} + MFD)$ and Q_{NPV}.

[17] The internal rate of return is defined as the interest rate r which makes the net present value of the investment equal to zero. As in the calculation of the *IRR*, the scale of the investment is not taken into account, the maximization of the internal rate of return corresponds to the selection of the investment characterized by the minimum risk associated with possible future increases of the discount rate r. From this perspective, choosing the capacity which maximizes the *IRR* corresponds to the selection of the least risky choice among the infinite possible alternatives with different capacities in the range $[0, \infty)$. The *IRR* can be implicitly computed using equation (19) and using the definition of $\hat{r}$ as

$$\frac{1}{IRR}\left(1 - \frac{1}{(1+IRR)^n}\right) = \frac{C(Q)}{R_1(Q)}. \tag{22}$$

It can be demonstrated that maximizing *IRR* is equivalent to minimizing $\widehat{IRR} = \frac{1}{IRR}\left(1 - \frac{1}{(1+IRR)^n}\right)$, and hence the optimal design flow is obtained by computing $d\widehat{IRR}/dQ$ through equations (12), (16), (18) and (22) and setting it equal to zero. The resulting equation is reported below only in the case when $MFD = 0$:

$$\underbrace{\frac{\eta_M D(Q) + \eta_0\, \alpha_0 Q\, D'(\alpha_0 Q) + \int_{\alpha_0}^{\alpha_M} \left(\frac{\eta_M - \eta_0}{\alpha_M - \alpha_0}\right) Q\, x^2\, D'(Qx)dx}{\eta_M Q\, D(Q) + \int_{\alpha_M}^{1} \eta_M\, Q^2\, x\, p(Qx)dx + \int_{\alpha_0}^{\alpha_M} \left[\frac{\eta_M - \eta_0}{\alpha_M - \alpha_0}\,(x - \alpha_0) + \eta_0\right] Q^2\, x\, p(Qx)\, dx}}_{f_{IRR}} = \underbrace{\frac{b}{Q}}_{g_{IRR}}. \tag{23}$$

The general expression can be obtained by adding the *MFD* to the arguments of the functions D, D' and p. The value assumed by the capacity Q_{IRR} maximizing the *IRR* can be studied by drawing the two curves defining the left-hand side (f_{IRR}) and the right-hand side (g_{IRR}) of equation (23). However, due to the predominance of the first terms at the numerator and the denominator in the left-hand side of the equation, the shape of the functions f_{IRR} and g_{IRR} is similar, making the choice of the optimal capacity in most cases extremely uncertain (see Figure 7b).

4. Case Study

[18] The analytical method developed in sections 2 and 3 has been tested through the application to an actual hydropower project recently proposed in northeastern Italy (Veneto Region, http://www.regione.veneto.it/Ambiente+e+Territorio/Ambiente/VIA/Progetto+74+2011.htm). The proposed plant should exploit the streamflows of Valfredda Creek, a small tributary of Biois Creek, belonging to the Piave River catchment, which is one of the major Alpine catchments of northern Italy (for a detailed description of the Piave River the reader is referred to *Botter et al.* [2010]). The catchment area at the planned intake of the hydropower plant is about 4 km^2, and the catchment elevations range from 3003 to 1753 m above sea level.

[19] Streamflow measurements along Valfredda Creek are completely lacking, making extremely uncertain the estimate of the underlying flow duration curve. According to the documentation available on line, the flow duration curve of Valfredda Creek has been estimated by the project designer with a monthly temporal resolution through an empirical method which is detailed below. Monthly runoff coefficients have been calculated for the catchment at hand starting from rainfall and streamflow data available in the

period 1992–2008 in a nearby catchment characterized by similar climatic and morphological features. On this basis, mean monthly discharges have been calculated by applying the above runoff coefficients to the rainfall time series observed in a meteorological station located in the Valfredda catchment, suitably aggregated at monthly time intervals. Given the empirical nature of the above method, and the large time scale employed for the estimate, the duration curve used by the project designers could be significantly biased, especially for the highest flows (daily/hourly data would be required to better describe the duration curve of the catchment). The focus of the paper, however, is not on the estimate of FDCs in ungauged sites, but rather on the relationship between the shape of the FDC and the optimal plant capacity. Hence, we decided to take into account the estimate of the FDC provided by the designer, in order to have a term of comparison for the analytical optimization performed later.

[20] The reliability of the estimate of the FDC provided in the project has been further assessed through the comparison with an independent estimate of the FDC of Valfredda Creek based on the analysis of the daily streamflows observed in Cordevole Creek at Saviner (which is a nearby subcatchment of the Piave River) from 1990 to 2008. Provided that the shape of the pdf of the specific (per unit area) discharge has been shown to be quite uniform in different reaches of the upper Piave catchment [*Botter et al.*, 2010], we estimated the FDC of the Valfredda Creek by rescaling the discharges observed at Saviner according to the ratio between the corresponding contributing areas, and calculating the exceedance probability of the rescaled flows. The two estimates of the FDC of Valfredda Creek are represented in Figure 5 (dots and diamonds, respectively). Figure 5 shows the general agreement between the two different estimates provided, except that for the extreme flows where the estimate based on daily data is obviously more accurate.

[21] Before applying the analytical optimization, the estimated streamflow pdf's have been fitted with a Gamma distribution. Even though other types of distributions are available, recent studies [*Botter et al.*, 2007, 2008] have shown that the emergence of Gamma streamflow pdf's is theoretically related to the ubiquitous Poissonian nature of the rainfall forcing. A Gamma distribution with shape parameter 3 and scale parameter 27 s m^{-3} was found to be the best approximation of the FDC estimate provided in the project. The same gamma function was also found to be in substantial agreement with the FDC estimated on the basis of the daily streamflow data collected in the Cordevole river. Accordingly, the duration curve of the Valfredda Creek has been approximated by a regularized gamma function of parameters 3 and 27 q (see Figure 5), which has then been used in the forthcoming computations.

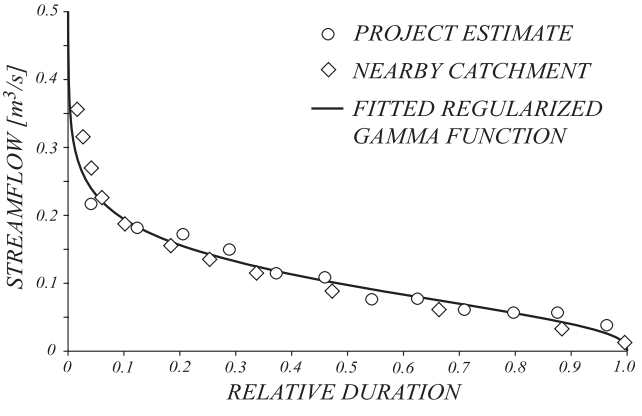

Figure 5. Flow duration curve of Valfredda Creek at the planned intake reported in the project (circles), estimate of the FDC of Valfredda Creek based on the analysis of the daily streamflows observed in Cordevole Creek at Saviner from 1990 to 2008 (diamonds), and fitted regularized gamma function (solid line).

[22] The estimated average streamflow is 0.11 m^3 s^{-1}, and the minimum flow discharge in the considered reach has been fixed by the Water Authority as $MFD = 0.025$ m^3 s^{-1} (23 % of the mean annual flow). The gross hydraulic head available between the intake and the outflow is about 200 m, suggesting the use of a Pelton turbine. The major technical and economic parameters characterizing the plant are listed in Table 1. In particular, the parameters defining the cost function C (equation (18)) have been chosen by setting $b = 0.6$ (see section 3), and calculating a from the overall estimated costs of the planned plant ($\sim 10^6$ euros).

[23] The optimal design flow for the maximization of the energy produced by the plant (Q_{EN}) has been derived from the intersection between the functions f_{EN} and g_{EN} at the two sides of equation (14) (section 2), as shown in Figure 6. The plot reinforces the difference in the order of magnitude of the two functions above, which significantly constrains the ordinate of the interception between the curves, and hence the duration of Q_{EN} (section 2). The corresponding optimal design flow Q_{EN} is equal to 0.24 m^3 s^{-1}, a streamflow value which has a relative duration of 0.04 (15 days). The degree of exploitation of the available water resources allowed by the optimal design flow is very high, as evidenced by the underlying water exploitation index, representing the fraction of the streamflows processed by the plant, which is equal to 0.75.

[24] The design flow which maximizes the NPV of the project (Q_{NPV}) is detected through a graphical method (Figure 7a), studying the intersections between the functions f_{NPV} (the marginal proceeds) and g_{NPV} (the marginal costs) of equation (20). The plot evidences the different behavior of the two curves, and the weak variability of g_{NPV} in the relevant range of Q, suggesting the robustness of the approximate method given by equation (21) in this

Table 1. Technical and Economic Parameters Characterizing the Hydropower Project Considered in the Case Study

Parameter	Value
MFD (m^3 s^{-1})	0.025
H (m)	203.20
α_0	0.1
α_M	0.3
η_0	0.75
η_M	0.89
n	15
r	0.045
$\hat{r}$	10.74
e_p (€/kW h)	0.22
a (€/$(m^3/s)^b$)	3.12×10^6
b	0.60

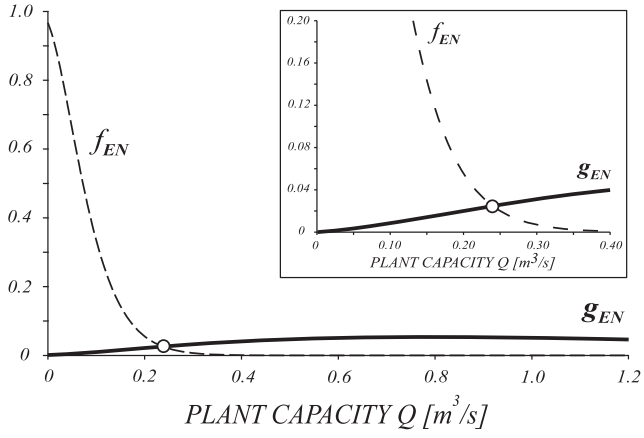

Figure 6. Graphical representation of the left-hand side ($f_{EN}(Q)$, dashed line) and of the right-hand side ($g_{EN}(Q)$, solid line) of equation (14). The optimal design flow stands at the intersection between f_{EN} and g_{EN} (circle) and turns out to be equal to 0.24 m^3 s^{-1}, a flow value which has a duration of 0.04 (15 days).

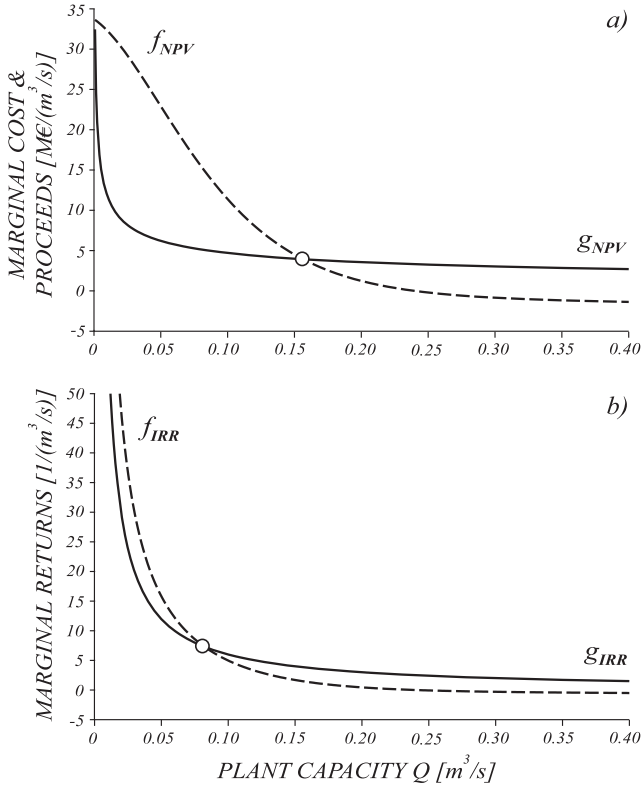

Figure 7. (a) Graphical representation of the left-hand side ($f_{NPV}(Q)$, dashed line) and of the right-hand side ($g_{NPV}(Q)$, solid line) of equation (20). The optimal design flow stands at the intersection between f_{NPV} and g_{NPV} (circle) and turns out to be equal to 0.16 m^3 s^{-1}, a flow value which has a duration of 0.19 (70 days). (b) Same as Figure 7a, but for the case of the *IRR* (equation (23)). The optimal design flow in this case turns out to be equal to 0.08 m^3 s^{-1}, a flow value which has a duration of 0.62 (226 days).

case. Moreover, the value of Q_{NPV} is almost insensitive to small variations of b around the reference value of 0.6, a circumstance that has been observed in all other simulations shown in the paper. The value of Q_{NPV} in the considered case study is 0.16 m^3 s^{-1}, noticeably smaller than Q_{EN}. The corresponding duration of the design flow maximizing the *NPV* is 0.19 (70 days).

[25] The design flow which maximizes the internal rate of return of the project (Q_{IRR}) can be analogously detected analyzing the intersection of the two curves defining the left-hand side (f_{IRR}) and the right-hand side (g_{IRR}) of equation (23) (Figure 7b). The design flow Q_{IRR} which results from the maximization of the *IRR* in the considered case study is 0.08 m^3 s^{-1}, a capacity which has a duration equal to 0.62 (226 days). As long as the additional wealth of the investment is neglected, Q_{IRR} is smaller than Q_{NPV}. The maximization of the *IRR*, however, leads to optimal values of the internal rate of return being much higher than the current discount rate, suggesting that the assumption $NPV = 0$ should not be considered realistic. Note also that, due to the similar shape displayed by the functions f_{IRR} and g_{IRR}, the optimum design flow is found to be very sensitive to the exponent b of the cost function. This suggests that a more detailed analysis of the costs is recommended when the internal rate of return is optimized.

[26] In Figure 8 and Table 2 the durations of the different optimal plant capacities resulting from the maximization of E (0.04), *NPV* (0.19) and *IRR* (0.62) are compared with the duration of the actual design flow resulting from the executive project of the plant (0.22, 80 days). The (positive) difference between the design flow maximizing the energy produced by the plant and the design flow optimizing economic indices suggests that the economic optimization of the plant is not able to guarantee an optimal exploitation of the water resources, as suggested by the observed decrease of the underlying exploitation indexes (from 0.75 to 0.7 and 0.5). The design flow derived from the optimization of the *NPV* of the project ($Q = 0.16$ m^3 s^{-1}), which has been shown to be the most effective of the two economic evaluation methods presented, is found to be in agreement with

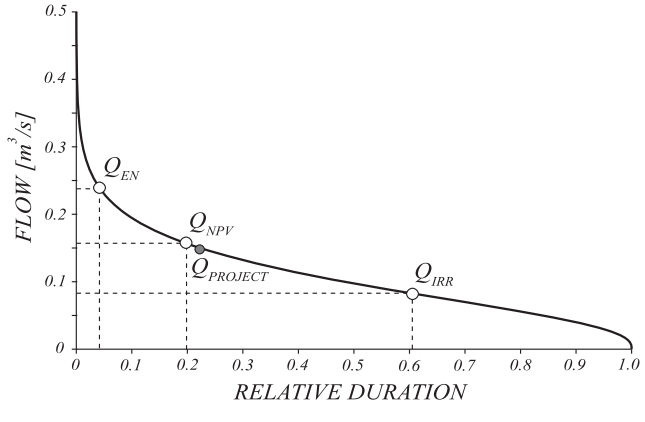

Figure 8. Durations of the different optimal plant capacities resulting from the maximization of energy (0.04), *NPV* (0.19), and *IRR* (0.62) compared with the duration of the actual design flow resulting from the executive project of the plant (0.22). The solid line represents the flow duration curve of Valfredda Creek at the planned intake.

Table 2. Actual Project Data and Results From the Proposed Analytical Method Applied to the Case Study

	Q (m^3 s^{-1})	$D(Q)$	E (kW h yr^{-1})	R_1 ($\times 10^6$ €)	C ($\times 10^6$ €)	NPV ($\times 10^6$ €)	IRR
Project	0.15	0.22	1.10×10^6	0.24	1		
Energy	0.24	0.04	1.19×10^6	0.26	1.33	1.50	0.18
NPV	0.16	0.19	1.14×10^6	0.25	1.03	1.67	0.23
IRR	0.08	0.62	0.87×10^6	0.19	0.70	1.36	0.27

the actual design flow of the project ($Q = 0.15$ m^3 s^{-1}), which has been set assuming a fixed duration for the optimal capacity equal to 80 days, a subjective value chosen on the basis of the personal experience of the plant designer.

[27] The analytical method proposed has also been compared with the results of the numerical optimization based on the temporal sequence of streamflows observed in Cordevole Creek at Saviner (suitably rescaled) in the time period 1990–2004. The time series of workable flows, $q_w(t)$, has been obtained from the incoming streamflows $q(t)$, for different plant capacities, by means of the rules discussed in section 2. The energy produced during every year has been calculated using equation (1) (with $\Delta T = 1$ year). The overall energy is then obtained as the sum of the annual energy produced by the plant during 15 years. The *NPV* has been calculated as $R_n(Q) - C(Q)$ (see equation (19)), with $C(Q)$ computed according to equation (18) and $R_n(Q) = \sum_{k=1}^{n} [1/(1+r)^k] R_1(Q)$. In this case the annual revenue $R_1(Q)$ is allowed to vary year by year because it depends on the streamflows actually processed during the considered year. Finally, the *NPV* is computed for different interest rates r unless the value of r for which the *NPV* is null (i.e., the *IRR*) is found. The procedure is repeated for different plant capacities Q. The behavior of E, *NPV* and *IRR* as a function of the plant capacity Q is shown in Figure 9. The optimal capacities in all the three cases are in substantial agreement with the results of the analytical model, reinforcing the robustness of the proposed approach.

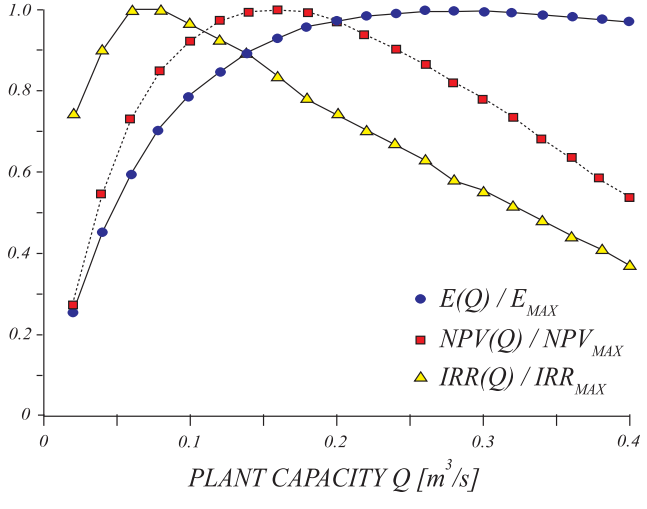

Figure 9. Results of the numerical optimization based on the temporal sequence of streamflows observed at Saviner (suitably rescaled) in the time period 1990–2004. The curves represent the produced energy (dots), the net present value (squares), and the internal rate of return (triangles) as a function of the capacity Q. Each curve has been normalized with respect to its maximum (indicated as E_{MAX}, NPV_{MAX}, and IRR_{MAX}, respectively).

5. Discussion

[28] In order to evidence the potential of the analytical approach developed, in this section we investigate the impact of the streamflow regime on the energy and economic optima of a power plant, and discuss some relevant implications in terms of economics and decision making.

[29] To explore the dependence of the value of $D(Q_{EN})$ on the hydrologic regime and the minimum flow discharge, in Figure 10 we show the dependence of $D(Q_{EN})$ on the coefficient of variation of the incoming streamflow pdf CV_q for different values of the *MFD* (for Pelton turbines). The curves have been evaluated via equation (14) assuming Gamma distributed incoming flows. Figure 10 confirms that in all cases $D(Q_{EN}) < 0.05$, as discussed in sections 2 and 4 using theoretical arguments. In particular, when the *MFD* is negligible, $D(Q_{EN})$ is minimum for regimes characterized by a limited variability of the flows. $D(Q_{EN})$ initially grows for $CV_q < 1$, and then slowly decreases for $CV_q > 1$. The maximum of $D(Q_{EN})$ for intermediate regimes is explained by analyzing the expected impact of CV_q on the intersection between f_{EN} and g_{EN} in equation (14): when the variability of q is low, g_{EN} has a pronounced peak, but it can intersect f_{EN} only after the peak, when g_{EN} is very close to zero; conversely, when the variability of q is large, g_{EN} is relatively low and flat, hence constraining the ordinate of the intersection between f_{EN} and g_{EN}. For intermediate variability instead, the intersection takes place when g_{EN} is approximately equal to its maximum value, leading to increased durations of the optimal capacity Q_{EN}. The presence of the *MFD* weakly changes the above picture only for CV_q smaller than 1. Nonnegligible *MFD*s determine an increase of

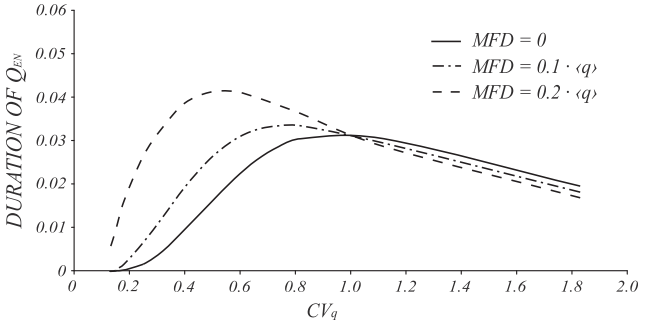

Figure 10. Impact of the streamflow variability (represented by the coefficient of variation of the streamflows CV_q) and the *MFD* (expressed as a fraction of the mean streamflow $\langle q \rangle$) on the duration of the energy optimal design flow Q_{EN}.

$D(Q_{EN})$ because in these circumstances $D(Q_{EN} + MFD)$ becomes sensibly smaller than $D(Q_{EN})$.

[30] In Figure 11 we explore how the plant capacity which maximizes the NPV and its duration are impacted by different streamflow regimes and different cost/revenue functions. For the sake of simplicity in this plot we set $MFD = 0$, $b = 0.6$, and $e_p = 0.22$€/kW h (the energy price currently prescribed by the Italian law). Instead of plotting the functions f_{NPV} and g_{NPV}, we plot $f^*_{NPV} = \theta f_{NPV}$ (solid lines) and $g^*_{NPV} = \theta g_{NPV}$ (dotted lines), where $\theta^{-1} = \hat{r} e_p H \rho g \eta_P \eta_M$. In physical terms, f^*_{NPV} represents the dimensionless marginal revenue (and behaves similarly to the duration curve of the inflows), while g^*_{NPV} is the ratio between the marginal costs and the annual revenues derived from processing a unit flow with the maximum efficiency. This representation has the advantage of separating the effect of hydrological processes (now imbedded in the function f^*_{NPV}) from that of economic parameters (included in g^*_{NPV}). The circles indicate the intersections between f^*_{NPV} and g^*_{NPV}, whose x coordinates represent Q_{NPV}. The plot shows the behavior of f^*_{NPV} for two different flow regimes ($CV_q = 0.8$ and $CV_q = 1.2$) and the behavior of g^*_{NPV} in correspondence of different ratios a/θ (dotted lines). Also indicated (shadowed dots) are the points corresponding to the optimization of the energy produced by the plant. The graph shows that $D(Q_{NPV})$ does not depend significantly on hydrologic attributes, rather it is mainly controlled by economic factors. The difference between Q_{EN} and Q_{NPV}, instead, is strongly dependent on both hydrological and economic features, provided that $Q_{EN} - Q_{NPV}$ increases significantly when the ratio a/θ increases (e.g., increased costs, decreased energy prices) and when the streamflow variability increases. Hence, especially for highly variable regimes, the optimal economic exploitation of the plant does not allow for the optimal exploitation of the available water resources. A decrease of the ratio a/θ would be required to get an economically feasible increase in the degree of exploitation of the available water resources (Figure 11). This goal could be obtained thanks to state incentives through two complementary policy strategies: (1) an increase of the energy price for renewable sources e_p; (2) a partial/total recovery of the costs that need to be sustained for the plant construction (either via the decrease of a or through a change of the shape of the marginal cost function). The second strategy should be preferred due to the implied reduced costs for the government. For instance, to move the economic optimum from the point A (0.21 $m^3\ s^{-1}$) to the point B (0.26 $m^3\ s^{-1}$) in Figure 11, an increase of e_p up to 0.44 €/kWh is required, which leads to an increase of the overall expense for the government equal to 3.60×10^6 euros. On the other hand, the same result could be achieved by decreasing the costs (i.e., reducing a via state incentives), with an overall expense of 0.66×10^6 euros. Note that, unless targeted state incentives driven by plant capacity are introduced, the energy optimum can never be achieved through price policies (because an infinite value of e_p would be required). Price policies pose some concerns also when remodulations of the energy prices are required. For instance, in the coming years the Italian government will probably lower the price of the energy from renewable hydroelectric plants e_p to reduce the related costs. Figure 12 shows that the proposed redefinition of e_p would modify the NPV of new and existing plants introducing a significant bias which penalizes the plants built on rivers characterized by highly variable discharges. The plot shows the percent decrease of NPV as a function of the percent decrease of e_p for plants exploiting river flows characterized by a different degree of variability. The solid lines refer to the case where the capacity is chosen to optimize the NPV with the current prices, assuming that a plant may be completed before the change of e_p and forced to operate under the new regime. The dashed lines, instead, refer to plants whose capacity is chosen to optimize the NPV with the modified price regime. The plot shows that the decrease of NPV for plants exploiting more variable discharges is always larger than that of plants which exploit weakly variable streamflows. Moreover, the graph shows that for highly variable flows the plants designed before the change of the energy price would experience a nonnegligible extra loss of NPV with respect to the plants designed after the price change, which is due to the change of the optimal design flow Q_{NPV} produced by the new price regime.

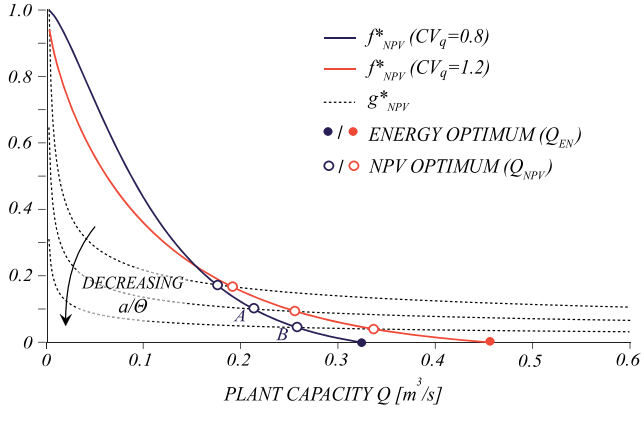

Figure 11. Impact of different streamflow regimes and different cost-revenue functions on the plant capacity maximizing the NPV and its duration.

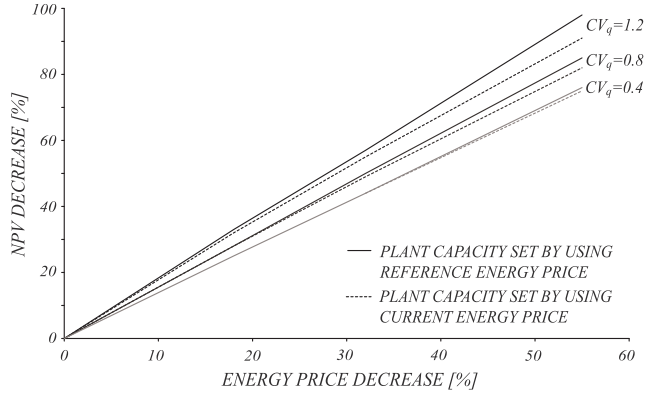

Figure 12. Percent decrease of NPV as a function of percent decrease of the energy price e_p. Three different regimes characterized by different streamflow variability are considered: $CV_q = 0.4$ (light gray lines), $CV_q = 0.8$ (dark gray lines), and $CV_q = 1.2$ (black lines). The solid lines refer to the case of plant capacities optimized by using reference energy prices, while the dotted lines refer to the case of plant capacities optimized considering current (lower) energy prices.

6. Conclusions

[31] The analytical model developed in the paper consists of a set of analytical expressions for the design flow which maximizes the produced energy and the profitability of a run-of-river plant. Such expressions can be easily applied to different hydrologic/economic contexts, or further simplified to provide immediate estimates of the duration of the optimal capacity of a plant. The robustness of the method, as well as its flexibility and generality, makes it a useful tool for selecting the optimal design flow in practical application, as demonstrated by the case study presented in the paper. The model developed also helps in identifying the hydrologic and economic controls on the optimal capacity of a plant. The duration of the energy optimum is shown to be typically below 0.05, but its specific value chiefly depends on the underlying streamflow variability. The streamflow regime also impacts the value of the capacity which maximizes the net present value of a plant, but not its duration, which mainly depends on economic features. The ease of application of the method makes it a valuable tool for scenario analysis and decision making. In particular, the paper discusses some limitations inherent in price policies by showing that uniformly subsidizing the energy prices to increase the degree of exploitation of available water resources is not convenient because of the huge costs implied. Plants which exploit highly variable water flows are shown to be less energy efficient than the plants exploiting more constant flows, and they are more sensitive to possible redefinitions of the energy price. As such, we suggest they should be better protected through state incentives. More in general, the study evidences the need for more targeted state actions taking into account the plant size and differentiated strategies depending on the hydrologic regime of a river.

Appendix A: Mathematical Details

[32] The derivative of equation (6) is

$$\frac{dE}{dQ} = \Delta T H \rho g \eta_P \eta_M \left\{ \frac{d}{dQ} \left[\int_{\alpha Q}^{Q} p(q_w + MFD)\, q_w\, dq_w \right] + \frac{d}{dQ}[Q\, D(Q + MFD)] \right\}. \tag{A1}$$

Using the Leibniz integral rule to calculate the first derivative at the right-hand side of equation (A1), we obtain

$$\frac{dE}{dQ} = \Delta T H \rho g \eta_P \eta_M [Qp(Q + MFD) - \alpha^2 Qp(\alpha Q + MFD) + D(Q + MFD) - Qp(Q + MFD)]. \tag{A2}$$

Note that the argument of the integral in equation (A1) does not depend on Q. Hence, its derivative is equal to zero and does not appear in equation (A2). When the first and fourth terms inside the square brackets are reduced, equation (A2) gives

$$\frac{dE}{dQ} = \Delta T H \rho g \eta_P \eta_M [D(Q + MFD) - \alpha^2 Qp(\alpha Q + MFD)]. \tag{A3}$$

Finally, recalling that the derivative of the flow duration curve with respect to Q equals the opposite of the streamflow probability density function (and hence $D'(\alpha Q + MFD) = -\alpha\, p(\alpha Q + MFD)$), we obtain

$$\frac{dE}{dQ} = \Delta T H \rho g \eta_P \eta_M [D(Q + MFD) + \alpha Q\, D(\alpha Q + MFD)] \tag{A4}$$

which is equation (7).

[33] The derivative of equation (11) can be computed in a similar manner. In particular,

$$\frac{dE}{dQ} = \Delta T H \rho g \eta_P \left\{ \frac{d}{dQ} \left[\int_{\alpha_M Q}^{Q} \eta_M p(q_w + MFD) q_w dq_w \right] + \frac{d}{dQ}[\eta_M Q D(Q + MFD)] + \frac{d}{dQ} \left[\int_{\alpha_0 Q}^{\alpha_M Q} \left(\frac{q_w - \alpha_0 Q}{\alpha_M Q - \alpha_0 Q} (\eta_M - \eta_0) + \eta_0 \right) p(q_w + MFD) q_w dq_w \right] \right\}. \tag{A5}$$

Using the Leibniz integral rule to calculate the first and the last derivatives at the right-hand side of equation (A5), we obtain

$$\begin{aligned} \frac{dE}{dQ} = \Delta T H \rho g \eta_P \Bigg\{ & \eta_M Q p(Q + MFD) - \eta_M \alpha_M^2 Q p(\alpha_M Q + MFD) \\ & + \eta_M D(Q + MFD) - \eta_M Q p(Q + MFD) + \frac{\eta_M - \eta_0}{\alpha_M - \alpha_0} \\ & \Bigg[\alpha_M^3 Q p(\alpha_M Q + MFD) - \alpha_0^3 Q p(\alpha_0 Q + MFD) \\ & - \int_{\alpha_0 Q}^{\alpha_M Q} \frac{1}{Q^2} q^2 p(q + MFD) dq \Bigg] - \frac{\eta_M - \eta_0}{\alpha_M - \alpha_0} \alpha_0 [\alpha_M^2 Q p(\alpha_M Q + MFD) \\ & - \alpha_0^2 Q p(\alpha_0 Q + MFD)] + \eta_0 [\alpha_M^2 Q p(\alpha_M Q + MFD) \\ & - \alpha_0^2 Q p(\alpha_0 Q + MFD)] \Bigg\}. \end{aligned} \tag{A6}$$

Reducing the first and fourth terms inside the braces at the right-hand side of the above equation, after grouping and reordering the other terms, equation (A6) gives

$$\begin{aligned} \frac{dE}{dQ} = \Delta T H \rho g \eta_P \Bigg\{ & \eta_M D(Q + MFD) - \frac{\eta_M - \eta_0}{\alpha_M - \alpha_0} \\ & \int_{\alpha_0 Q}^{\alpha_M Q} \frac{q^2}{Q^2} p(q + MFD) dq + p(\alpha_M Q + MFD) \alpha_M^2 Q \\ & \left(-\eta_M + \alpha_M \frac{\eta_M - \eta_0}{\alpha_M - \alpha_0} - \alpha_0 \frac{\eta_M - \eta_0}{\alpha_M - \alpha_0} + \eta_0 \right) + p(\alpha_0 Q + MFD) \\ & \left(-\alpha_0^3 Q \frac{\eta_M - \eta_0}{\alpha_M - \alpha_0} + \alpha_0^3 Q \frac{\eta_M - \eta_0}{\alpha_M - \alpha_0} - \alpha_0^2 \eta_0 Q \right) \Bigg\}. \end{aligned} \tag{A7}$$

Finally, reducing the terms within the round brackets of the above equation and changing the integration variable of the integral, equation (A7) becomes

$$\frac{dE}{dQ} = \Delta T H \rho g \eta_P \left[\eta_M D(Q + MFD) + \eta_0 \alpha_0 Q D'(\alpha_0 Q + MFD) + \int_{\alpha_0}^{\alpha_M} \left(\frac{\eta_M - \eta_0}{\alpha_M - \alpha_0} x \right) Q x D'(Q x + MFD)\, dx \right] \tag{A8}$$

which is equation (12).

[34] **Acknowledgments.** The authors thank the Complex Unit VIA of the Veneto Region for providing data related to the case study. Yuen Ting Bess Lam and Behnam Doulatyari are gratefully acknowledged for their comments and suggestions on the language. Financial support from the research project Progetto di Ateneo 2010, CPDA105501/10 (Impatto del regime idrologico sulle dinamiche trofiche in ecosistemi fluviali), is also acknowledged.

References

Aggidis, G. A., E. Luchinskaya, R. Rothschild, and D. C. Howard (2010), The costs of small-scale hydro power production: Impact on the development of existing potential, *Renewable Energy*, *35*, 2632–2638, doi:10.1016/j.renene.2010.04.008.

Anagnostopoulos, J. S., and D. E. Papantonis (2007), Optimal sizing of a run-of-river small hydropower plant, *Energy Convers. Manage.*, *48*, 2663–2670, doi:10.1016/j.enconman.2007.04.016.

ARCADIS (2011), Hydropower generation in the context of the EU WFD, report, Dir. Gen. for Environ., Eur. Comm., Brussels.

Botter, G. (2010), Stochastic recession rates and the probabilistic structure of stream flows, *Water Resour. Res.*, *46*, W12527, doi:10.1029/2010WR009217.

Botter, G., A. Porporato, I. Rodriguez-Iturbe, and A. Rinaldo (2007), Basin-scale soil moisture dynamics and the probabilistic characterization of carrier hydrologic flows: Slow, leaching-prone components of the hydrologic response, *Water Resour. Res.*, *43*, W02417, doi:10.1029/2006WR005043.

Botter, G., S. Zanardo, A. Porporato, I. Rodriguez-Iturbe, and A. Rinaldo (2008), Ecohydrological model of flow duration curves and annual minima, *Water Resour. Res.*, *44*, W08418, doi:10.1029/2008WR006814.

Botter, G., S. Basso, A. Porporato, I. Rodriguez-Iturbe, and A. Rinaldo (2010), Natural streamflow regime alterations: Damming of the Piave River basin (Italy), *Water Resour. Res.*, *46*, W06522, doi:10.1029/2009WR008523.

Bozorg Haddad, O., M. Moradi-Jalal, and M. A. Mariño (2011), Design-operation optimisation of run-of-river power plants, *Proc. Inst. Civ. Eng. Water Manage.*, *164*, 463–475.

Da Deppo, L., C. Datei, V. Fiorotto, and A. Rinaldo (1984), Capacity and type of units for small run-of-river plants, *J. Int. Water Power Dam Constr.*, *36*(10), 33–38.

European Small Hydropower Association (1998), Guida all'idroelettrico minore. Per un corretto approccio alla realizzazione di un piccolo impianto, *Rep. DG XII-97/010*, Dir. Gen. for Energy, Eur. Comm., Brussels.

Fahlbuch, F. (1983), Optimum capacity of a run-of-river plant, *J. Int. Water Power Dam Constr.*, *35*(3), 25–37.

Fahlbuch, F. (1986), Optimum capacity and tunnel diameter of run-of-river plants, *J. Int. Water Power Dam Constr.*, *38*(5), 42–55.

Freeman, M. C., C. M. Pringle, and C. R. Jackson (2007), Hydrologic connectivity and the contribution of stream headwaters to ecological integrity at regional scales, *J. Am. Water Resour. Assoc.*, *43*(1), 5–14.

Gordon, J. L. (1981), Estimating hydro stations costs, *J. Int. Water Power Dam Constr.*, *33*, 31–33.

Gordon, J. L. (1983), Hydropower costs estimates, *J. Int. Water Power Dam Constr.*, *35*, 30–37.

Gordon, J. L., and C. R. Noel (1986), The economic limits of small and low-head hydro, *J. Int. Water Power Dam Constr.*, *38*, 23–26.

Gordon, J. L., and A. C. Penman (1979), Quick estimating techniques for small hydro potential, *J. Int. Water Power Dam Constr.*, *31*, 46–55.

Kaldellis, J. K., D. S. Vlachou, and G. Korbakis (2005), Techno-economic evaluation of small hydro power plants in Greece: A complete sensitivity analysis, *Energy Policy*, *33*, 1969–1985.

Montanari, R. (2003), Criteria for the economic planning of a low power hydroelectric plant, *Renewable Energy*, *28*, 2129–2145.

Najmaii, M., and A. Movaghar (1992), Optimal design of run-of-river power plants, *Water Resour. Res.*, *28*(4), 991–997.

Ogayar, B., and P. G. Vidal (2009), Cost determination of the electro-mechanical equipment of a small hydro-power plant, *Renewable Energy*, *34*, 6–13, doi:10.1016/j.renene.2008.04.039.

Paish, O. (2002), Small hydro power: Technology and current status, *Renewable Sustainable Energy Rev.*, *6*, 537–556.

Papantonis, D. (2001), *Small Hydro Power Stations*, Simeon, Athens.

Poff, N. L., J. D. Olden, D. M. Merritt, and D. M. Pepin (2007), Homogenization of regional river dynamics by dams and global biodiversity implications, *Proc. Natl. Acad. Sci. U.S.A.*, *104*(14), 5732–5737.

Pringle, C. M. (2001), Hydrologic connectivity and the management of biological reserves: A global perspective, *Ecol. Appl.*, *11*(4), 981–998.

Santolin, A., G. Cavazzini, G. Pavesi, G. Ardizzon, and A. Rossetti (2011), Techno-economical method for the capacity sizing of a small hydropower plant, *Energy Convers. Manage.*, *52*, 2533–2541, doi:10.1016/j.enconman.2011.01.001.

Tharme, R. E. (2003), A global perspective on environmental flow assessment: Emerging trends in the development and application of environmental flow methodologies for rivers, *River Res. Appl.*, *19*, 397–441.

Vogel, R. M., and N. M. Fennessey (1995), Flow duration curves II: A review of applications in water resources planning, *J. Am. Water Resour. Assoc.*, *31*(6), 1029–1039.

Voros, N., C. Kiranoudis, and Z. Maroulis (2000), Short-cut design of small hydroelectric plants, *Renewable Energy*, *19*, 545–563.

Zolezzi, G., A. Bellin, M. C. Bruno, B. Maiolini, and A. Siviglia (2009), Assessing hydrological alterations at multiple temporal scales: Adige River, Italy, *Water Resour. Res.*, *45*, W12421, doi:10.1029/2008WR007266.